

# Learning new perception–action solutions in virtual ball bouncing

Antoine H. P. Morice · Isabelle A. Siegler ·  
Benoît G. Bardy · William H. Warren

Received: 7 June 2006 / Accepted: 23 February 2007 / Published online: 21 March 2007  
© Springer-Verlag 2007

**Abstract** How do humans discover stable solutions to perceptual-motor tasks as they interact with the physical environment? We investigate this question using the task of rhythmically bouncing a ball on a racket, for which a passively stable solution is defined. Previously, it was shown that participants exploit this passive stability but can also actively stabilize bouncing under perceptual control. Using a virtual ball-bouncing display, we created new behavioral solutions for rhythmic bouncing by introducing a temporal delay (45°–180°) between the motion of the physical racket and that of the virtual racket. We then studied how participants searched for and realized a new solution. In all delay conditions, participants learned to maintain bouncing just outside the passively stable region, indicating a role for active stabilization. They recovered the approximate initial phase of ball impact in the virtual racket cycle (half-way through the upswing) by adjusting the impact phase with the physical racket. With short delays (45°, 90°), the impact phase quickly shifted later in the

physical racket upswing. With long delays (135°, 180°), bouncing was destabilized and phase was widely visited before a new preferred phase gradually emerged, during the physical downswing. Destabilization was likely due to the loss of spatial symmetry between the ball and physical racket motion at impact. The results suggest that new behavioral solutions may be discovered and stabilized through broad irregular sampling of variable space rather than through a systematic search.

**Keywords** Bouncing ball · Virtual reality · Intermodal perception · End-to-end latency · Dynamical regimes

## Introduction

Adaptive behavior can be understood as emerging from the interaction between an agent and its environment, characterized in terms of the perception–action cycle (Warren 2006). The two systems are coupled mechanically, through forces exerted by the agent, and informationally, through optic, acoustic, and haptic variables. When the agent performs an action, forces are applied that change the state of the environment in accordance with the laws of physics, and generate new information in accordance with the laws of optics, acoustics, haptics, and so on (Gibson 1979). Reciprocally, this information is used to regulate the forces that the agent applies to the environment, in accordance with laws of control for a given task. These interactions give rise to the dynamics of behavior, with attractors that correspond to preferred stable behavioral solutions (Saltzman and Kelso 1987). Such stabilities reflect the constraints of the agent–environment system, including the physics of the environment, the biomechanics of the body, sensory information, and the demands of the task.

---

A. H. P. Morice · I. A. Siegler (✉)  
UPRES EA 4042 Contrôle Moteur et Perception,  
Univ Paris Sud 11, 91405 Orsay Cedex, France  
e-mail: isabelle.siegler@u-psud.fr

B. G. Bardy  
Institut Universitaire de France, 103 bd St Michel,  
75005 Paris, France

B. G. Bardy  
Motor Efficiency and Deficiency Laboratory,  
University Montpellier-1, 700 Avenue du Pic Saint Loup,  
34090 Montpellier, France

W. H. Warren  
Department of Cognitive and Linguistic Sciences,  
Brown University, Box 1978, Providence, RI, USA

The task of rhythmically bouncing a ball on a racket provides a deceptively simple but conceptually rich model system that incorporates all of these constraints, allowing us to investigate the dynamics of perception and action. Ball bouncing provides a case study for the general problem of how people learn stable behavioral solutions to everyday tasks as they interact with the physical environment, from manipulating tools and other objects to learning skills such as skiing or cycling. Within this framework we can address such questions as to what properties define a behavioral attractor, how agents capitalize on the physics of the world to organize behavior, whether behavior is passively stable or actively controlled, and how information is exploited in the process. In the present study, we seek to understand how humans interacting with a physical system discover a new attractor and use it to stabilize their behavior.

### Dynamics of ball bouncing

The dynamics of bouncing a ball on a racket was analyzed by Schaal et al. (1996) and Dijkstra et al. (2004), who demonstrated the existence of a passively stable region for 1D (vertical) bouncing. This passive stability regime occurs when a periodically moving racket hits the ball as the racket is decelerating, during the last quarter-cycle of upward motion. Specifically, a system with a coefficient of restitution  $\alpha$  and gravitational constant  $g$  is passively stable if racket acceleration at impact remains between 0 and a value of  $-2g(1 + \alpha^2)/(1 + \alpha)^2$ . For example, with  $\alpha = 0.5$  and  $g = 9.8 \text{ m/s}^2$ , racket acceleration must be in the negative range between 0 and  $-10.9 \text{ m/s}^2$ , corresponding to a phase of  $90^\circ$  to  $136.7^\circ$  (where  $0^\circ$  is defined as the lowest racket position); a Lyapunov stability analysis revealed a smaller region of maximal stability between  $-2$  and  $-5 \text{ m/s}^2$ . In this regime, small perturbations of ball velocity do not have to be actively corrected by racket adjustments to maintain stable bouncing, for the ball's trajectory will gradually relax back to a fixed point attractor at a constant impact acceleration (and bounce height) over the next several cycles. In contrast, if impact occurs during the preceding quarter-cycle of racket motion (between a phase of  $0^\circ$  and  $90^\circ$ ), when racket acceleration is positive, small perturbations will be amplified unless corrected by cycle-to-cycle racket adjustments, which requires more demanding active control. Thus, if participants take advantage of physical stability properties, one might expect that the maximally stable region would serve as a behavioral attractor, which is specified to the participant by minimum variability in impact acceleration, bounce height, or racket trajectory.

In experiments with a physical ball, Sternad et al. (2001a) found that the mean racket acceleration at impact

did indeed fall in the negative range on the large majority of trials, clustered about the maximally stable region. This suggests that humans discover the passively stable solution and that it acts as a behavioral attractor. Sternad et al. (2001b) also observed that over 40 practice trials, impact acceleration decreased toward maximally stable negative values, again suggesting that participants learn to exploit stability properties.

However, subsequent experiments using a virtual reality (VR) set-up have shown that novices can also maintain bouncing with positive impact accelerations with the physical racket, outside the passive stability range, presumably through a process of active stabilization (Siegler et al. 2003). In this set-up, participants move a physical racket that controls a virtual racket on screen in order to bounce a virtual ball, thereby allowing elasticity ( $\alpha$ ) or gravity ( $g$ ) to be easily manipulated. Note that it is the impact acceleration of the virtual racket when it meets the virtual ball that must be in the negative range for passively stable bouncing. Using such an apparatus, de Rugy et al. (2003) and Siegler et al. (2003) found that participants corrected for perturbations of the ball's trajectory due to changes in  $\alpha$  or  $g$  within one or two cycles—faster than possible through passive relaxation—by actively adjusting the racket period to match the new ball period in order to recover stability. Such results imply a mixed control regime combining passive stability and active stabilization to maintain bouncing.

In the present experiment, we used the VR set-up to investigate how participants learn a new behavioral solution for rhythmic bouncing. To create such a novel solution, we inserted various temporal delays between the physical and virtual rackets, such that the motion of the virtual racket lagged behind that of the physical racket by a fixed time interval. For example, in order to hit the ball during the virtual racket's upswing, impact might have to occur during the physical racket's downswing. Adding a delay thus shifted the passive stability region to a different phase in the physical racket cycle, providing a means to study how participants search for and realize a new stable perceptual-motor solution, which may combine passive and active stabilization.

### Adaptation and learning a shifted attractor

In studies of interlimb coordination, evidence of attractive states was originally discovered for in-phase ( $0^\circ$ ) and anti-phase ( $180^\circ$ ) coordination modes (Kelso et al. 1981; Yamanishi et al. 1980). Subsequently, Zanone and Kelso (1992, 1997) demonstrated that, with training, other stable phases could also be learned, with the time required to stabilize a new coordination mode depending on the imposed relative phase. Consistent with the view that

coordination dynamics has an informational basis (Kelso 1994, 1995), it was recently found that rapid learning of new coordination patterns was facilitated for movements with visual spatial symmetries, even when the new patterns were complex or involved non-homologous muscles (Mechsner et al. 2001). The reliability of purely perceptual judgments of relative phase and phase variability also reflects the stability of in-phase and anti-phase motion, both visually (Bingham et al. 1999; Schmidt et al. 1990; Zaal et al. 2000) and haptically (Wilson et al. 2003). Moreover, haptic information can serve to stabilize new coordination modes (Kelso et al. 2001). These results suggest that similar effects on pattern stability and learning rate may be observed when stabilizing a new relative phase that is not imposed but a discovered solution for a perceptual coupling with the physical environment.

The delay in the presentation of visual feedback has been identified as acting like a control parameter that can induce phase transitions in perceptual-motor behavior (Tass et al. 1996). Transitions between several different regimes of phasing were observed during sinusoidal forearm tracking with delayed visual feedback. This dynamical framework suggests the study of adaptation to new behavioral solutions induced by delaying the visual consequences of movement. By doing so, the classical attractive states of relative phase and their stability properties can be expected for 45°, 90°, 135° and 180° relative phasing induced by time delays. As found in Zanone and Kelso's (1992) experiments, pattern stability should increase with learning. More specifically, as the mean observed phase shifts toward the learning pattern, the frequency distribution of exhibited relative phases should progressively sharpen and the relaxation time should become shorter.

#### Time delays and human performance

An unavoidable aspect of current VR technology and other human-machine interfaces is an “end-to-end latency” (commonly called “time delay” or “time lag”), which refers to the time elapsed between the occurrence of a physical event, such as the displacement of an object by the user, and its perceptual consequences in the virtual environment (Adelstein et al. 1996; Wenzel 1998). The existence of a time delay has two related consequences: it alters the spatio-temporal congruence between different sensory modalities (e.g., between proprioception during arm motion and the visual/acoustic consequences) and it also imposes new physical constraints that may require adjustments in the spatio-temporal pattern of perceptual-motor behavior (e.g., the timing of arm motion with respect to ball motion).

The introduction of delayed feedback has become a common paradigm to investigate the capacity of human observers to adapt to new intersensory temporal relationships. Cunningham et al. (2001) reported behavioral evidence that the human visuo-motor system can adapt to new intersensory temporal relationships. In their experiment, participants used a mouse to maneuver a small airplane through a field of obstacles on a computer monitor. In the pre- and post-test phases, the plane motion lagged behind the mouse motion by the minimum value of 35 m s. In the training phase, visual feedback was delayed by an additional 200 m s. Participants did not perform well at the start of training, but at the end of the training, most participants were able to navigate the obstacle field at roughly the same speed as in the normal condition. Cunningham et al. also observed a negative aftereffect during the post-test, indicating that visuo-motor adaptation had occurred. The authors concluded from this study that “the internal delay inherent in intersensory integration can be altered”, which helps to understand how the brain may be able to combine multisensory information with various modality-dependent processing times.

Intersensory delays induce some form of intersensory spatial offset, depending on the time course of velocity and direction of motion. When motion is periodic, some regularities might occur in this spatial offset. Langenberg et al. (1998) showed that during forearm tracking of a sinusoidally moving target with different visual delays, temporal and spatial incompatibility influence tracking performance differentially. For all the different target frequencies, tracking error revealed a cyclic behavior with an increase up to delays of about 50% of the target cycle duration and an improvement for delays larger than 50% (with a relative delay of 50%, arm and target motion were moving in opposing direction). The authors found that for sinusoidal tracking, the phase delay and spatial relationships were of greater importance for the quality of tracking than the absolute time delay.

In the present work, adding time delays in the bouncing task forced participants to use the (perceptual) consequences of their arm movements on the ball's trajectory to stabilize their behavior on a new perceptual-motor solution, within the task constraints. Different delays, yielding different relative phases between the physical and virtual rackets (45°, 90°, 135°, 180°), were tested with separate groups of participants. By doing so, we created new solutions that participants had to “find” during a learning session. Similar to the work of Langenberg et al. (1998), effector motion was close to sinusoidal. Therefore, we expected that the four spatio-temporal regularities would differentially influence the process of discovering new behavioral solutions.

To summarize, the present study pursued two aims: (1) to assess whether participants are able to adjust their visuomotor coordination in order to achieve new a behavioral solution, and (2) if so, to characterize the time course of these adjustments and the routes taken during the learning process.

## Materials and methods

### Participants

Participants were 29 novice volunteers (26 right-handed, 3 left-handed). They were informed about the experimental procedure, which was approved by local committee, and signed a consent form. Four experimental groups, balanced for number, gender and age, were constituted ( $n = 7$ , 2 females and 5 men, mean age  $29 \pm 6$  years;  $n = 7$ , 3 females and 4 men, mean age  $29 \pm 6$  years;  $n = 7$ , 2 females and 5 men, mean age  $31 \pm 8$  years;  $n = 8$ , 3 females and 5 men, mean age  $25 \pm 1$  years).

### Virtual reality apparatus and data collection

Participants stood upright in front of a large screen (2.70 m wide  $\times$  1.25 m high) at a distance of 1.5 m from it and held a table tennis racket in their preferred hand (Fig. 1). The racket, which will be referred to as “the physical racket”, could be moved freely in three dimensions. However, during the experiment, participants were asked to keep it horizontal and to perform movements in the vertical dimension only. A sheet of cardboard positioned horizontally at neck level prevented them from seeing the racket once the experiment began. The racket position was measured by an electromagnetic sensor [Flock of Birds (FOB), Model 6DFOB<sup>®</sup>, Ascension Technologies] at a sampling rate of 120 Hz. The Flock of Bird sensor was fixed on the backside of the physical racket. The plastic screw used to

fix the FOB sensor was located exactly at 0.2 m from the tip of the racket handle. The transmitter base of the FOB (serving as a space reference) was positioned in such a way that the sensor was directly facing it. The position signal was sent (RS-232 communication port) to custom-written experimental software in the host computer (MS Windows XP Pro<sup>®</sup>, bi 2.6GHz Pentium processor, 512 Mo RAM, graphic engine PCI ATI Technologies, 9600 Sapphire Radeon). From the vertical position signal of the physical racket, the software computed online the position of a “virtual racket”, displayed as a horizontal bar, whose displacement (1D vertical) was displayed on the screen (Open GL Graphics, resolution equal to  $800 \times 600$  pixels) with a LCD projector (50 Hz, see Fig. 1). The software also computed online both the position of a virtual ball visible on the screen and the interactions between the virtual racket and the ball. Therefore, by manipulating the physical racket, participants controlled the motion of the virtual racket used to bounce the virtual ball. A sound was played each time an impact between the virtual racket and ball occurred. Ball (diameter = 0.04 m), coefficient of restitution ( $\alpha = 0.50$ ) and gravity ( $g = 9.81 \text{ m/s}^2$ ) remained constant during the entire experiment.

In studies of this type, it is essential to accurately measure the end-to-end visual latency. This visual lag of our VR apparatus was accurately measured at 2,000 Hz with an analog setup. A 1D accelerometer (Entran<sup>®</sup> EGAS—FS-5) fixed onto the physical racket next to the sensor was used to detect the initiation of the real racket motion. A photodiode (Burr—Brown OPT301) was positioned close to the screen where the virtual racket was displayed at its initial position and was used to detect the beginning of the virtual racket motion. The visual lag measured was the elapsed time from input human motion until the immediate consequences of that input in the display and was found to be  $37.3 \pm 11.1 \text{ m s}^{-1}$ .<sup>1</sup> A temporal gain on this value was obtained by implementing an 8.3-m s polynomial predictive regression<sup>2</sup> in our software. A second method was needed to measure ETEL, in presence of the predictive filter. We used a digital video camera (sampling rate = 50 Hz, de-interlaced) to record simultaneously the displacement of both physical and virtual rackets. This second test-bed provided a 2 m s accuracy

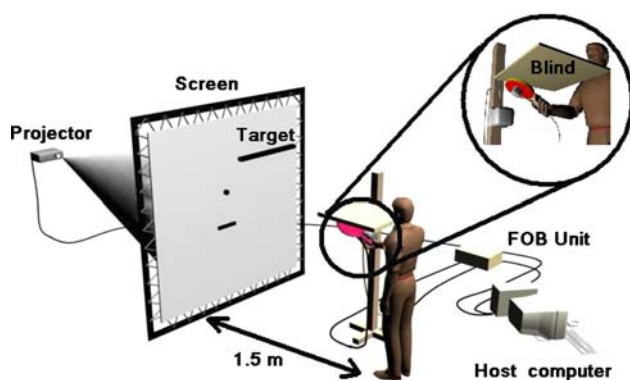


**Fig. 1** Virtual reality set-up for ball bouncing used in the experiment

<sup>1</sup> The variability in the latency measurement is caused by an incompatibility between the Flock of Bird (120 Hz) and the video-projector (50 Hz) update rates, coupled with a lack of synchronization between the two components.

<sup>2</sup> Instead of correcting the overall 37.3 m s end-to-end latency of our VE, we chose to correct only 8.3 m s with a predictive polynomial regression because this 8.33 m s predictive filter leads to the minimal error in the approximation of the physical racket positions and velocities (mean position error =  $0.0005 \pm 0.0013 \text{ m}$ ; mean velocity error =  $0.2925 \pm 0.1278 \text{ m s}^{-1}$ ).



(by an interpolation from 20 m s period sample), and served as a routine check. This second step allowed us to insure an intrinsic lag of  $29.73 \pm 1.07$  m s. Therefore, given that participants had to bounce the ball with an imposed period of 670 m s, the minimal end-to-end latency corresponded in fact to  $16^\circ$  of relative phase ( $\Delta\phi$ ) between physical and virtual racket.

### Procedure, design and experimental conditions

Before the experiment began, participants were asked to keep the racket in their preferred hand at a comfortable height (elbow flexed approximately at  $90^\circ$ ). This racket position was measured and taken as a zero/reference position. During a trial, participants were asked to hit the virtual ball with the racket and to maintain this rhythmic bouncing action for the entire duration of the trial. Bouncing had to be such that after each impact the ball came as close as possible to a virtual target that was presented as a horizontal line on the screen 0.55 m above zero position. To facilitate consistent bouncing periods, a computer-generated metronome signal (beep frequency 670 m s i.e., 1.5 Hz) was used to prescribe the racket cycle period. Moreover, by enforcing a constant racket period, the metronome ensured that the intrinsic end-to-end latency corresponded to a constant phase lag between the physical and virtual racket displacements. Participants were instructed to synchronize the timing of impact with the metronome beeps throughout the entire trial. Each trial lasted 40 s and included approximately 60 cycles and impacts. Trials began with the ball appearing on the right side of the screen and rolling on a horizontal line extending to the middle of the screen. When the ball reached the end of the line, it dropped toward the racket. The horizontal position of the virtual racket was fixed and centered under the drop position of the ball. This starting procedure was designed to visually prepare the participants for the beginning of a trial (de Ruyg et al. 2003). To limit fatigue, a short rest period was introduced after every ten trials during which feedback about the performance was given to the participants, in terms of mean and standard deviation of signed error (defined as the distance between ball peak position and target height).

### Experimental design

Each participant took part in three experimental sessions, spread out over 2 days. In Session 1 (day 1), participants performed 50 identical trials in a normal condition (i.e., with mean lag between physical and virtual rackets of 29.73 m s). During Session 2 (50 trials, performed on day 2), an additional lag was purposely added to the intrinsic

lag in order to obtain an overall lag resulting in specific relative phases between physical and virtual rackets. These overall lags created different temporal congruencies between physical movements and visual information (the visual impact occurring after the expected physical impact). Each group experienced a particular relative phase ( $\Delta\phi$ ) between the physical racket and the virtual racket, created by the introduction of a specific value of the overall lag:  $45^\circ$  of relative phase for the first group (lag of 83.75 m s),  $90^\circ$  for the second group (167.5 m s),  $135^\circ$  for the third group (251.25 m s), and  $180^\circ$  for the last group (335 m s).

Typical bounce sequences representing racket and ball cycles during Session 2 are plotted in Fig. 2 in order to illustrate how the introduction of various time-lags generates different relative phases between the rackets and consequently influences the impact point in both the physical and virtual racket cycles. If the participant does not adjust his/her movements and tries to hit the ball near the end of the physical racket's upward swing, the impact with the virtual racket would occur significantly earlier in the virtual cycle, and hence, frequently during its downward swing. Consequently, in order to successfully bounce the ball on the virtual racket, participants were expected to adjust their movements so as to hit the ball later in the physical racket cycle (specifically,  $45^\circ$ ,  $90^\circ$ ,  $135^\circ$  or  $180^\circ$  later) so that the ball would impact the virtual racket with appropriate timing. The predicted phase in the physical racket cycle at impact is  $\phi_P = \phi_V +$  relative phase between both rackets. Assuming that the virtual racket impact occurs in the last half of the virtual upswing, participants were expected to "hit" the ball when the physical racket was moving downward in the  $90^\circ$ ,  $135^\circ$  and  $180^\circ$  delay conditions, as illustrated in Fig. 2c, d. Finally, Session 3 occurred on day 2 immediately after Session 2, and replicated the Session 1 condition with 25 trials. The three sessions were always presented in the same order. The entire experiment consisted of 125 trials and lasted approximately for 2 h 30 s.

### Data reduction and analyses

Initial data processing was performed online by the host computer on the FOB position signal (moving average on ten preceding samples and fourth order polynomial regression with the prediction of one position sample ahead). During post processing, the first 8 s and the last bounce of each trial were excluded from data treatment. Raw data of racket positions were filtered with a second-order Butterworth filter with a cutoff frequency of 12 Hz. Filtered racket position values were symmetrically differentiated to yield racket velocity and then differentiated again to obtain racket acceleration. Several variables were

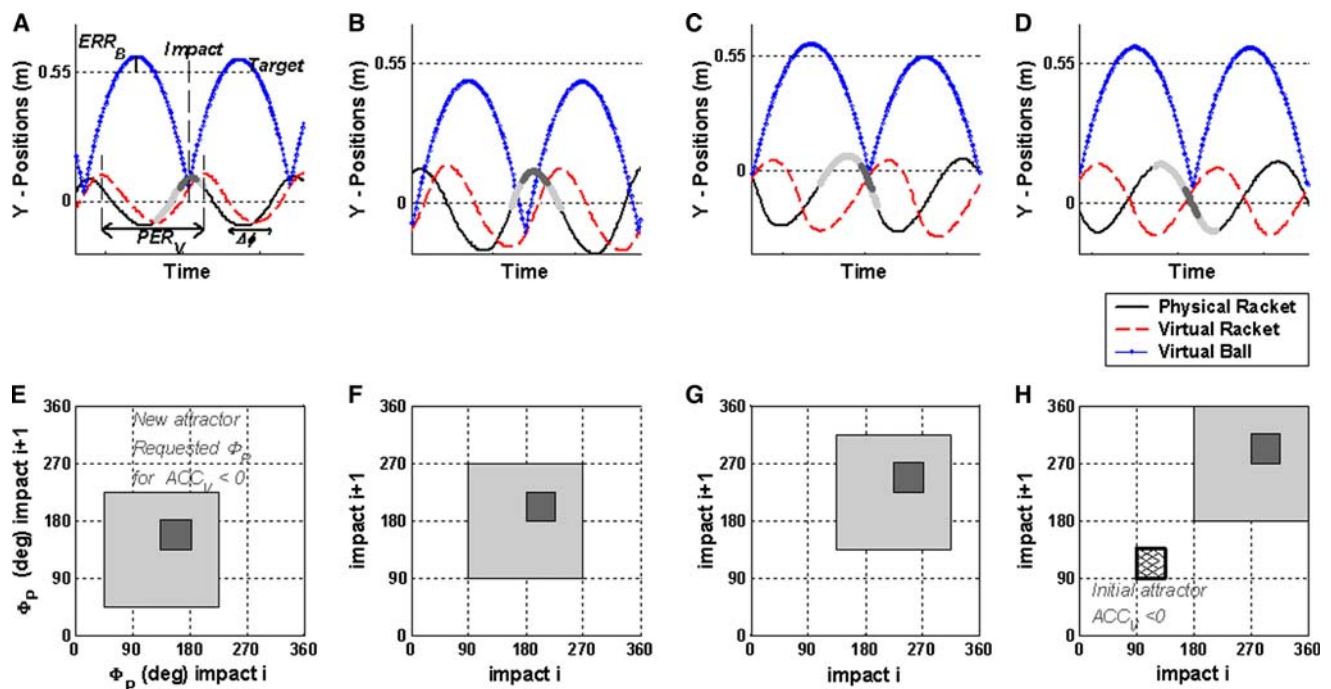


**Fig. 2** Illustration of new passive and active control regions introduced in Session 2. Plots **a–d** depict sample trials of bounce sequences showing the pattern after adaptation to the four lag conditions, or relative phase between physical and virtual rackets (**a** = 45°, **b** = 90°, **c** = 135° and **d** = 180°). Plot **a** illustrates the computation of the dependent variables  $ERR_B$  (bouncing error) and  $PER_V$  (period of virtual racket). The new passive and active control regions are shown on the physical racket (**a–d**) by **bold dark** (46.7° long) and **light grey** lines (180° long), respectively. Plots **e–h** illustrate the associated first-return maps ( $\phi_p$  of impact  $i+1$  as a

function of  $\phi_p$  of impact  $i$ ). **Dark grey squares** (46.7° × 46.7°) illustrate the new [passively stable, i.e., acceleration of the virtual racket at impact ( $ACC_V < 0$ )] sensori-motor attractors in each condition (**a** = 45°, **b** = 90°, **c** = 135° and **d** = 180°). **Light grey squares** (180° × 180°) indicate the related active control regions ( $ACC_V > 0$ ), and correspond to the first half cycle of the virtual racket. The hatched 46.7° × 46.7° square located on the *bottom left corner* of plot **h** shows the original passive stability attractor evidenced by Schaal et al. (1996)

computed to capture the task performance and the impact behavior.

Task performance variables included the period of the virtual racket ( $PER_V$ ) and the bounce error ( $ERR_B$ ).  $PER_V$  at each cycle was calculated as the time (s) separating consecutive maximum positions of the virtual racket.  $ERR_B$  was calculated as the distance (m) between the target height and the peak of the ball trajectory following either the single impact in the virtual racket cycle or the last impact in cases of multiple impacts within one cycle.

Impact variables included velocity ( $VEL_V$ ), and acceleration ( $ACC_V$ ) of the virtual racket at impact, the impact phase in the physical racket cycle ( $\phi_p$ ), and the impact phase in the virtual racket cycle ( $\phi_v$ ). In cases of multiple impacts within a given racket cycle, these variables were computed only for the first impact in the cycle. To be consistent with previous studies (Sternad et al. 2001a; de Rugy et al. 2003) a virtual racket cycle was defined as the racket motion between two maximum positions of the virtual racket. Furthermore, with this definition, the occurrence of first impacts in the downward motion of

virtual racket would be recorded; these are indicative of how perturbed the participants were in presence of the added lag, and how they progressively responded to it. In contrast, a physical racket cycle was defined as the racket motion between two minimum positions of the physical racket. Impacts were expected to occur later in the physical racket cycle as lag increased, shifting from upward racket motion (for the 45° and 90° groups) to downward motion (for the 135° and 180° groups), and performance was expected to improve throughout Session 2. By defining the physical racket cycle in this way, we made it possible to observe a shift in the location of impacts within the physical racket cycle. For each cycle, racket velocity and position values were centered and normalized and plotted in the phase plane (racket velocity as a function of racket position). The impact phase  $\phi$  in a physical or virtual racket cycle was defined as the phase angle (in degrees) of impact in the phase plane  $\phi = 180 - \arctan(VEL_R/Y_R)$ . With this convention,  $\phi$  was equal to 0° at minimum racket position and equal to 180° at maximum racket position for both the physical and the virtual racket.

## Statistical analyses

For all the dependent variables, mean values were first computed for each trial. Standard deviations were also calculated for each trial when within-trial variability was to be analyzed (e.g., bouncing error and racket acceleration at impact: SD-ERR<sub>B</sub> and SD-ACC<sub>V</sub>). These values were then averaged for each block of five trials, giving ten consecutive block values per participant (Newell et al. 1997; Eversheim and Bock 2001). One participant from the 135°-group and two participants from the 180°-group, were excluded from all analyses because of their inability to perform the bouncing task in Session 2.

### Assessing Group × Block effects

Two-way ANOVAs (blocks × groups) with repeated measures on the Block factor were conducted separately by means of all variables for Session 1, Session 2 and Session 3, respectively. The significance level was set at  $P = 0.05$ . These analyses aimed primarily at assessing whether there were group differences in the rate of change in performance during the sessions.

### Assessing time course of learning

In order to characterize the time course of performance improvement, exponential regressions were fitted (by using Matlab nlinfit function) to group means of several variables across the ten blocks (one regression per group per variable) (Sternad et al. 2001b; Liu et al. 2003). When converging, fitting procedures (using least squares) returned three estimated parameters: the initial value  $V_1$ , the limit value  $V_L$  of exponential function ( $F = V_1 + (V_L - V_1) \exp^{-(\text{block}-1)/\tau}$ ) and the time constant  $\tau$ .  $\tau$  was the time constant to asymptotic performance (Liu et al. 2003). Convergence of fitting procedures and values of  $\tau$  gave an indication of whether the learning process was completed or not, and made it possible to compare qualitatively the changes in performance over time course in the four groups. Fitting procedures also returned the coefficient of determination  $r^2$ .

### Assessing learning quality

For each group, pairwise  $t$ -tests were conducted separately, based on the means of all variables to compare the five last trials of Session 1 and Session 2. The objective was to evaluate the participants' ability to recover at the end of Session 2 the initial behavior observed in Session 1. The significance level was set at  $P = 0.05$ .

## Assessing destabilization

For each group, pairwise  $t$ -tests were conducted separately, based on the means of all variables to compare the five last trials of Session 1 and the five first trials of Session 3. The objective was to evaluate the potential destabilization of natural bouncing behavior at the beginning of Session 3 due to the preceding learning phase in which delays were introduced. The significance level was set at  $P = 0.05$ .

## Results

### Session 1: normal spatio-temporal congruency [relative phase ( $\Delta\phi$ ) = 16°]

The data analysis in the first session served as a control for differences between groups. All participants performed exactly the same task and a similar behavior was thus expected across the four groups. ANOVAs yielded no significant main effect for group on (mean) PER<sub>V</sub> and ERR<sub>B</sub>, suggesting that the four groups produced similar bouncing performance. ANOVAs also yielded no significant main effect for group on (mean) VEL<sub>V</sub>, ACC<sub>V</sub> and  $\phi_V$ , indicating that the ball-racket impact behavior was also similar between groups. In Session 1,  $\phi_P$  was not studied, since it is very close to  $\phi_V$ .

Learning was found to occur in all groups and with the exception of  $\phi_V$ , for all performance variables and all impact variables. Separate ANOVAs (10 blocks × 4 groups) performed on PER<sub>V</sub>, ERR<sub>B</sub>, VEL<sub>V</sub>, and ACC<sub>V</sub> revealed a significant main effect of blocks,  $F_{(9,198)} > 2.59$ , all  $P < 0.05$ . No significant Group × Block interaction was found for any of the dependent variables,  $F_{(27,198)} < 1$ , all  $P > 0.05$ , indicating that behavioral changes at ball-racket impact were similar across groups (Table 1).

As the four groups did not exhibit significantly different behaviors, the data from all participants were pooled together. For all the dependent variables, the mean of the last block was taken to provide baseline values of performance in the normal (lag = 29.73 m s) condition, as presented in Table 2. The observed mean value of PER<sub>V</sub> ( $0.65 \pm 0.11$  s) in the last block was very close to the imposed value of 0.67 s, and that of ERR<sub>B</sub> ( $0.04 \pm 0.07$  m) was near the expected value of 0 m. The slightly positive value of ERR<sub>B</sub> indicates that participants overshot the target line by about 4 cm.

In order to assess the learning time constant  $\tau$  (expressed in trial block units) as well as the initial value and final asymptotic values, we looked for an exponential decay in ERR<sub>B</sub> and SD-ERR<sub>B</sub> as a function of block order (Fig. 3a). Exponential convergence was found for ERR<sub>B</sub> with a time

**Table 1** Statistical analysis performed on all mean block values for each dependent variable ( $PER_V$ ,  $ERR_B$ ,  $VEL_V$ ,  $ACC_V$ ,  $\Phi_V$ ) during the first session (Session 1)

Session	Effect	Performance		Behavior		
		$PER_V$	$ERR_B$	$VEL_V$	$ACC_V$	$\Phi_V$
Session 1	Group	$F(3,22) = 0.23$ , $P = 0.87$	$F(3,22) = 1.07$ , $P = 0.38$	$F(3,22) = 0.34$ , $P = 0.80$	$F(3,22) = 1.44$ , $P = 0.26$	$F(3,22) = 0.97$ , $P = 0.42$
	Learning	$F(9,198) = 4.24$ , $P = 0.00^*$	$F(9,198) = 5.53$ , $P = 90.00^*$	$F(9,198) = 2.60$ , $P = 0.01^*$	$F(9,198) = 4.21$ , $P = 0.00^*$	$F(9,198) = 0.90$ , $P = 0.53$
	Interaction	$F(27,198) = 1.25$ , $P = 0.19$	$F(27,198) = 0.82$ , $P = 0.72$	$F(27,198) = 0.96$ , $P = 0.53$	$F(27,198) = 0.87$ , $P = 0.65$	$F(27,198) = 0.74$ , $P = 0.82$
Pool	Learning	$F(9,225) = 4.08$ , $P = 0.00^*$	$F(9,225) = 5.83$ , $P = 0.00^*$	$F(9,225) = 2.63$ , $P = 0.01^*$	$F(9,225) = 4.17$ , $P = 0.00^*$	$F(9,225) = 0.82$ , $P = 0.59$

**Table 2** Last block means of within-trial means and standard deviation of virtual racket period ( $PER_V$ ) (s), signed bounce error ( $ERR_B$ ) (m), velocity at impact ( $VEL_V$ ) (m/s), acceleration at impact ( $ACC_V$ ) ( $m/s^2$ ), virtual and physical racket contact phase ( $\Phi_V$  and  $\Phi_P$ ) ( $^\circ$ ) for the three sessions

Conditions	Session 1		Session 2						Session 3			
	All participants		45°		90°		135°		180°		All participants	
	Mean	Within trial SD	Mean	Within trial SD	Mean	Within trial SD	Mean	Within trial SD	Mean	Within trial SD	Mean	Within trial SD
$PER_V$	0.65	0.11	0.66	0.10	0.70	0.14	0.65	0.14	0.65	0.13	0.64	0.10
$ERR_B$	0.04	0.07	0.05	0.06	0.07	0.26	0.09	0.12	0.04	0.22	0.04	0.07
$VEL_V$	1.05	0.14	1.07	0.12	0.98	0.43	0.88	0.54	0.99	0.49	1.04	0.13
$ACC_V$	3.18	5.38	3.64	5.20	8.69	7.82	0.97	7.92	-0.02	7.54	1.25	4.91
$\phi_V$	82.62	14.74	82.34	13.56	84.31	74.26	101.47	50.33	97.99	27.27	89.80	12.37
$\phi_P$	96.48	16.25	141.20	9.61	156.03	69.02	206.56	52.59	258.05	74.35	102.64	10.22

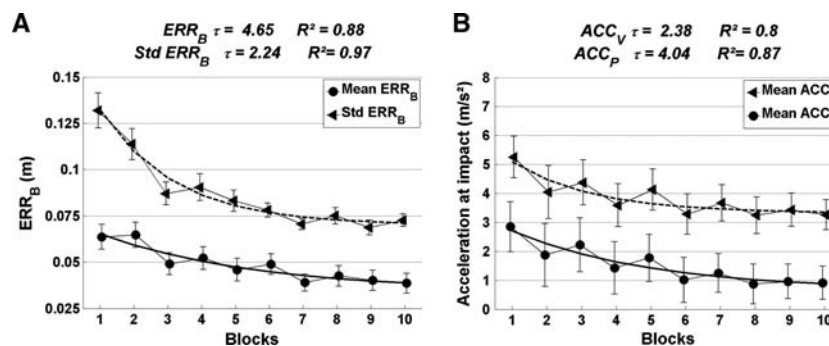


**Fig. 3** **a** Mean signed bounce error ( $ERR_B$ ) and standard deviation of signed bounce error ( $SD-ERR_B$ ) as a function of trial blocks for all participants ( $N = 26$ ) in the first 50 trials session. **b** Associated virtual racket acceleration at impact ( $ACC_V$ ) and standard deviation of

virtual racket acceleration at impact ( $SD-ACC_V$ ). Vertical bars represent standard errors of the individual block means. The solid line represents the exponential fit with corresponding  $\tau$  and  $r^2$  values

constant  $\tau$  of 4.65 blocks ( $r^2 = 0.88$ ) and for  $SD-ERR_B$  ( $\tau = 2.41$  blocks,  $r^2 = 0.96$ ), indicating that the mean error and within-trial variability decreased exponentially with learning (Fig. 3a). The asymptotic values of  $ERR_B$  and  $SD-ERR_B$  converged at 0.038 and 0.07 m.

The fitting procedure was also performed on mean racket acceleration at impact ( $ACC_V$ ) and within-trial

variability of racket acceleration at impact ( $SD-ACC_V$ ) (Fig. 3b).  $ACC_V$  showed an exponential decrease from an initial value of 5.11  $m/s^2$  to a final value of 3.28  $m/s^2$ , with a time constant  $\tau$  equal to 2.54 blocks ( $r^2 = 0.67$ ), and all  $ACC_V$  values were significantly different from 0  $m/s^2$ . The fit of  $SD-ACC_V$  also converged ( $\tau = 2.33$ ,  $r^2 = 0.67$ ). The passive stability regime with negative acceleration at



impact, previously found in normal bouncing (Sternad et al. 2001a), was not observed during Session 1:  $ACC_V$  was never in passive stability range of values ( $-10.9; 0 \text{ m/s}^2$ ). For the sake of discussion, we also computed the physical racket acceleration at impact, which decreased from  $2.85 \pm 6.07$  in block 1 to  $0.92 \pm 3.99 \text{ m/s}^2$  in block 10.

Results during the first learning session (Session 1) thus indicated that the four groups performed the task in similar ways. Behavioral changes were evidenced on all dependent performance and impact variables (except  $\phi_V$ ), and the number of trials was shown to be sufficient during this first session for participants to reach regular bouncing behavior and performances.

Session 2: new spatio-temporal congruency  
[relative phase ( $\Delta\phi$ ) =  $45^\circ, 90^\circ, 135^\circ, 180^\circ$ ]

In Session 2, time delays were introduced between physical and virtual rackets to create new relative phases of  $45^\circ$  to  $180^\circ$ , thus shifting the physical racket's impact phase for the stable regime of bouncing. The data analysis in the second session aimed at exploring the dynamics of learning such new stabilities.

*Task performance:  $ERR_B$  and  $PER_V$*

Figure 4 (left column) plots  $ERR_B$  block means for the four groups over all sessions, as a function of block. Whereas the  $45^\circ$  group has  $ERR_B$  values below 0.05 m with little change throughout Session 2, the  $90^\circ, 135^\circ,$  and  $180^\circ$  groups show a sharp change at the beginning of the session and continuous adaptation over the following blocks.

The ANOVA on  $ERR_B$  showed a significant Group  $\times$  Block interaction,  $F_{(27,198)} = 2.09, P < 0.05$ , indicating differences in adaptation between groups, although they converged at similar final values at the end of the session (within 0.05 m). Distinct adaptation dynamics are indicated by exponential fits of  $ERR_B$ , with time constants of  $\tau = 2.36$  blocks for the  $45^\circ$  group ( $r^2 = 0.68$ ),  $\tau = 1.74$  blocks for the  $90^\circ$  group ( $r^2 = 0.97$ ),  $\tau = 4.99$  for the  $135^\circ$  group ( $r^2 = 0.77$ ), and  $\tau = 2.64$  blocks for the  $180^\circ$  group ( $r^2 = 0.93$ ).

The ANOVA on  $PER_V$  also yielded a significant Group  $\times$  Block interaction,  $F_{(27,198)} = 2.35, P < 0.05$ . This effect is related to the fact that in some conditions participants had more difficulty following the metronome beeps at the beginning of Session 2 than in other conditions. Mean values of  $PER_V$  for the  $45^\circ$  and  $135^\circ$  groups remained constant at the expected value over the Session 2 (block 10:  $0.66 \pm 0.10 \text{ s}$  and  $0.65 \pm 0.14 \text{ s}$ ), whereas it was above the expected value in the  $90^\circ$  group (block 10:  $0.70 \pm 0.14 \text{ s}$ ). Values of  $PER_V$  for the

$180^\circ$  group ranged from  $0.59 \pm 0.15 \text{ s}$  at block 1 to  $0.65 \pm 0.13 \text{ s}$  at block 10.

*Ball-racket impact:  $VEL_V, ACC_V, \phi_P, \phi_V$*

The ANOVA on  $VEL_V$  at impact yielded a significant Group  $\times$  Block interaction,  $F_{(27,198)} = 3.30, P < 0.05$ . None of the groups recovered identical  $VEL_V$  values at the end of Session 2 when compared with the end of Session 1 (paired-samples  $t$ -test,  $N = 35, 35, 30, 30, t = -2.27, 2.41, 7.50, 3.66; df = 34, 34, 29, 29; P < 0.05$ ). Although  $VEL_V$  was expected to be equal to 1.05 m/s, final  $VEL_V$  values (last block of Session 2) were equal to 1.07, 0.96, 0.88, and 0.99  $\text{m/s}^2$  for the  $45^\circ, 90^\circ, 135^\circ$  and  $180^\circ$  groups, respectively. The  $45^\circ$  and  $180^\circ$  groups were therefore closer to the expected value than the  $90^\circ$  and  $135^\circ$  groups.

The ANOVA on  $ACC_V$  at impact (see Fig. 5) yielded a significant main effect of group,  $F_{(3,22)} = 19.21, P < 0.05$ , and a significant decrease over blocks,  $F_{(9,198)} = 6.15, P < 0.05$ , but no interaction,  $F_{(27,198)} = 1.20, P = 0.23$ . Comparison  $t$ -tests established that all  $ACC_V$  values for the  $45^\circ$  (except the two last block values) and  $90^\circ$  groups were positive and significantly different from  $0 \text{ m/s}^2$ . None of the  $ACC_V$  values for  $135^\circ$  and  $180^\circ$  were significantly different from  $0 \text{ m/s}^2$ . Final  $ACC_V$  values (last block of Session 2) were equal to 3.64, 8.69, 0.97 and  $-0.02 \text{ m/s}^2$  for the  $45^\circ, 90^\circ, 135^\circ$  and  $180^\circ$  groups, respectively. Participants in the  $90^\circ, 135^\circ$  and  $180^\circ$  groups did not recover identical  $ACC_V$  mean values at the end of Session 2, in comparison with the end of Session 1 (paired samples  $t$ -test,  $N = 35, 30, 30; t = -11.8, 5.15, 4.17; df = 34, 29, 29, P < 0.05$ ).

Figure 4 (right column) illustrates  $\phi_P$  (triangles) and  $\phi_V$  (circles) plotted as a function of block number for each of the four groups. At the end of the Session 2, the virtual impact phases in each group had recovered near to the pre-perturbation value of approximately  $90^\circ$ . This was accomplished by shifting the phase of the physical racket, such that by the end of Session 2,  $\phi_P$  had shifted by an amount that mostly (but not completely) compensated for the added delay. Given the observed  $\phi_V$  in the  $45^\circ, 90^\circ, 135^\circ,$  and  $180^\circ$  conditions, the expected values of  $\phi_P$  were  $127^\circ, 174^\circ, 236^\circ,$  and  $278^\circ$ , ( $\phi_P = \phi_V + \text{relative phase}$ ) and the observed values in the last block of Session 2 were  $141^\circ, 156^\circ, 206^\circ$  and  $258^\circ$ , respectively (Table 2). Thus, on average, impact occurred during the downswing of the physical racket in the  $135^\circ$  and  $180^\circ$  delay conditions. Inserts in Fig. 4 illustrate average phase planes of the virtual racket cycle at the end of the second experimental session produced by all participants in each experimental group. Racket trajectories are close to sinusoidal for all groups, although some deviation can be observed for the

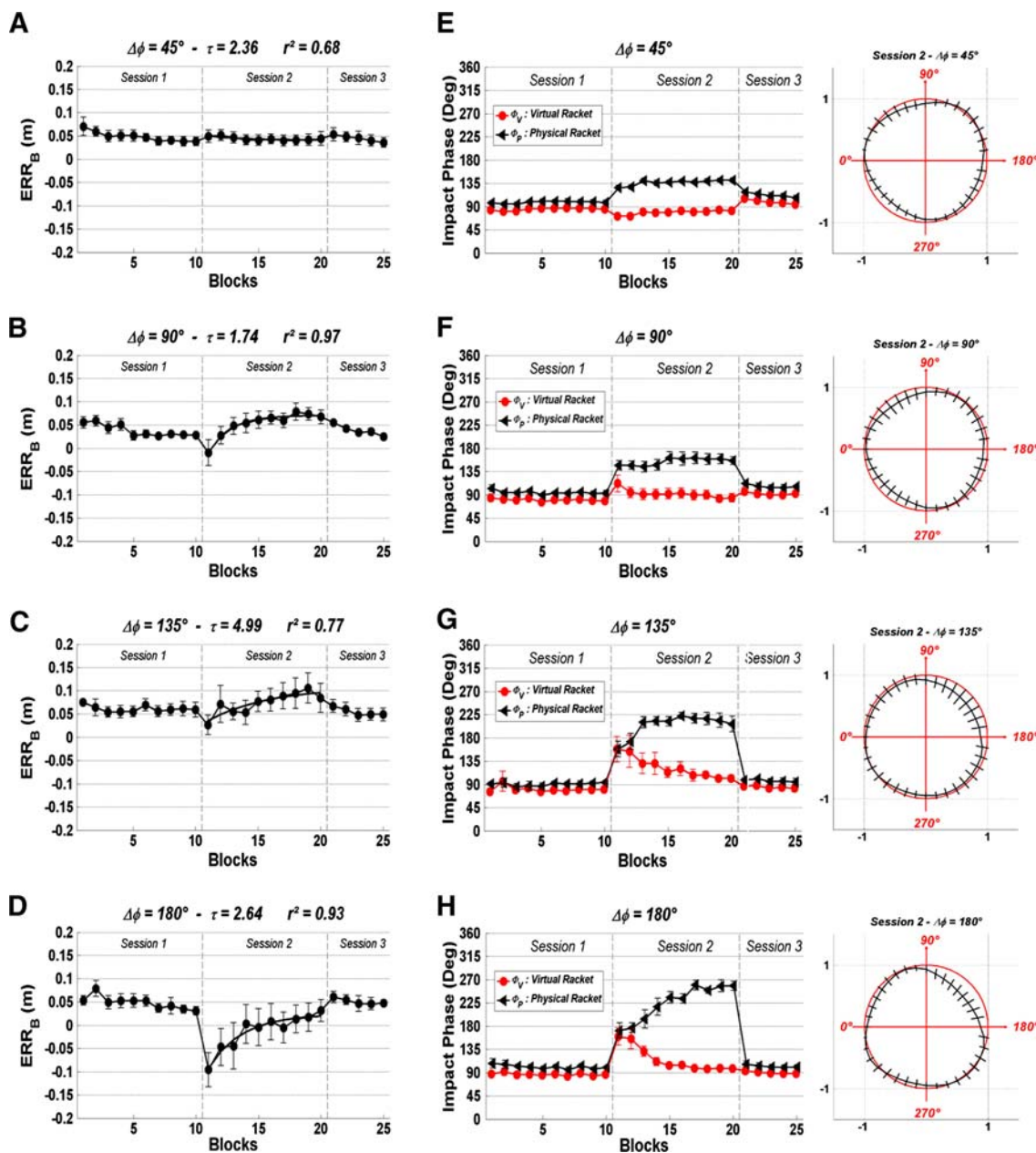


**Fig. 4** Left column (a–d plots): bounce error (ERR<sub>B</sub>) as a function of blocks for the four groups during the three sessions. Right column (e–h plots): virtual and physical racket impact phase ( $\Phi_P$ ,  $\Phi_V$ ) plotted as a function of trial block for the four groups. Vertical

bars represent standard errors of the individual block means. Insets show the mean phase plans of the virtual racket (and standard mean errors for each of the 36 parts of normalized racket cycles) at block 10 of the Session 2

180°-group, due to the changes in the physical racket when hitting the ball downward. However, racket trajectories appear to be sufficiently harmonic in all cases to make phase at impact a consistent dependent variable.

The different delay conditions yielded different adaptation times. ANOVAs revealed a significant group by block interaction for  $\phi_P$ ,  $F_{(27,198)} = 4.43$ ,  $P < 0.05$ , and  $\phi_V$ ,  $F_{(27,198)} = 2.91$ ,  $P < 0.05$ . The 45° and 90° groups adapted almost immediately to the new phase, whereas the 135° and 180° groups required multiple blocks for the virtual

phase to recover and the physical phase to stabilize. Indeed, while the 45° and 90° groups recovered mean  $\phi_V$  values at the end of Session 2 that were not different from the end of Session 1 (paired samples  $t$ -test,  $N = 35, 35$ ;  $t = 1.34$ ,  $-1.34$ ;  $df = 34, 34$ ;  $P > 0.05$ ), the final values for the 135° and 180° groups were slightly but significantly higher than at the end of Session 1 (paired samples  $t$ -test,  $N = 30, 30$ ;  $t = -5.53$ ,  $-4.36$ ;  $df = 29, 29$ ;  $P < 0.05$ ), suggesting that they had not completely adapted (see Table 2). Moreover, all groups displayed significant shifts in the mean  $\phi_P$  values

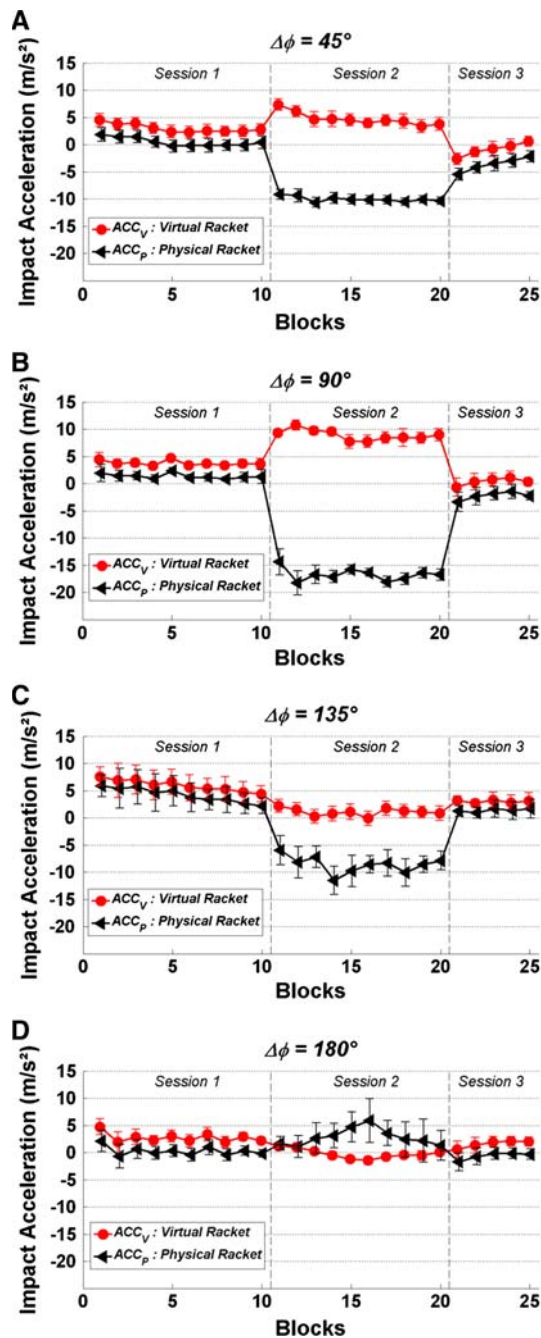


**Fig. 5** Virtual ( $ACC_V$ ) and physical ( $ACC_P$ ) racket acceleration at contact as a function of blocks for the four groups (a–d) during the three sessions. Vertical bars represent standard errors of the individual block means

at the end of Session 2 when compared with the end of Session 1 (paired samples  $t$ -test,  $N = 35, 35, 30, 30$ ;  $t = -24.36, -18.05, -14.74, -25.49$ ;  $df = 34, 34, 29, 29$ ;  $P < 0.05$ ).

Taken together, these results suggest that there were somewhat different patterns of adjustment to the different phase delays. The adaptation of  $VEL_V$ ,  $\phi_P$  and  $\phi_V$  differed

between the four groups, although that of  $ACC_V$  was quite similar (general decrease although to different values). Moreover, the four groups had different performance and ball-racket behavior at the end of Session 2. Separate ANOVAs (four groups) performed on mean values of  $PER_V$ ,  $VEL_V$ , and  $ACC_V$  in the last block revealed a significant difference between groups,  $F_{(3,126)} > 3.79$ , all  $P < 0.05$ .

#### Frequency distribution of $\phi_P$

To examine the process of adaptation more closely, we plotted histograms of  $\phi_P$  for the last block of Session 1 and the first five and last blocks of Session 2 (Fig. 6). Interestingly, these frequency distributions are either unimodal or relatively flat, but never appear bimodal. In the  $45^\circ$  and  $90^\circ$  delay conditions, a single peak shifted from near  $90^\circ$  at the end of Session 1 to new mean phases of  $141^\circ$  and  $156^\circ$  at the end of Session 2. In these two conditions, impact continued to occur during the upswing of the physical racket, a familiar behavior pattern. In contrast, in the  $135^\circ$  and  $180^\circ$  delay conditions, the unimodal peak vanished for the first two or three blocks of Session 2 and the distribution was spread over the full range of values, indicating the absence of a stable phase. Over the next several blocks, a separate peak emerged at new mean phases of  $206^\circ$  and  $258^\circ$ , respectively, and gradually sharpened up. This pattern suggests that the preferred phase in Session 1 was destabilized in Session 2, after which a new stable solution was discovered and homed in upon over multiple blocks. This is probably due to the fact that impact occurred during the downswing of the physical racket in these two conditions, requiring the stabilization of an unfamiliar and counterintuitive perceptual-motor coordination pattern.

Standard deviation of  $\phi_P$  within each block was also computed in order to give more insight into the evolution of phase distribution throughout learning. For the  $45^\circ$ -group, the SD of  $\phi_P$  was  $22.67^\circ$  in the first block of Session 2. At block 10, the SD of  $\phi_P$  was only  $13.71^\circ$ . The mean phase was adjusted almost immediately, such that  $\phi_P$  shifted by about  $45^\circ$  in the first block of five trials, with a tight distribution around  $90^\circ + 45^\circ$  that appears to shift only slightly thereafter. For the  $90^\circ$  group, the distribution is broader in block 1 with an SD of  $68.80^\circ$ . The unimodal peak immediately shifts from  $90^\circ$  to about  $135^\circ$ , and then gradually shifts to  $156^\circ$  and sharpens over successive blocks, but never reaches the expected value of  $90^\circ + 90^\circ$ . This indicates that the  $90^\circ$ -group did not adapt to the new delay as quickly as the  $45^\circ$ -group. In block 10, the SD of  $\phi_P$  was  $38.93^\circ$ .

The  $135^\circ$  and  $180^\circ$  groups displayed no preferred phase in the first few blocks but visited the full phase range. At the beginning of Session 2, the SDs of  $\phi_P$  were  $103.30$  and



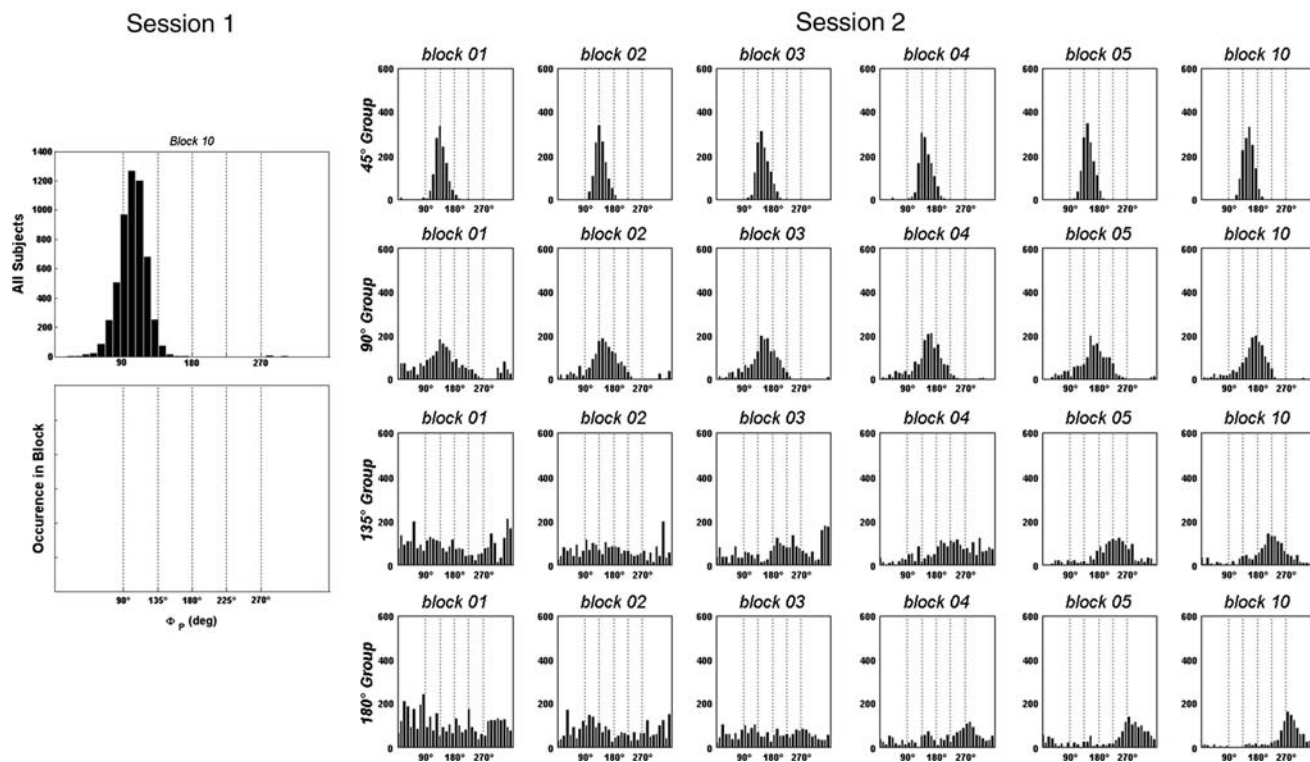


**Fig. 6** Distribution (all bounces and all participants pooled) of the physical racket impact phase ( $\Phi_p$ ) in some blocks across Session 2 (from left to right: first, second, third, fourth, fifth and last block of Session 2; from top to bottom: 45°, 90°, 135° and 180° groups)

103.28 for the 135° and 180° groups, respectively. A unimodal peak shapes up in block 3 or 4 and continues to sharpen through block 5. By block 10 these peaks are well defined but broader than in the above groups, with SDs of 59.65° and 60.09° for the 135° and 180° groups.

An ANOVA on the SD of  $\phi_p$  in Block 1 revealed a significant effect of group,  $F_{(3,22)} = 26.544$ ,  $P > 0.05$ , and Newman Keuls post-hoc tests showed that the dispersion was significantly smaller for the 45° and 90° groups than for the 135° and 180° groups. A similar ANOVA for Block 10 also showed a significant effect of group,  $F_{(3,22)} = 9.7023$ ,  $P > 0.05$ , and Newman Keuls post-hoc tests demonstrated that the dispersion of  $\phi_p$  was significantly smaller for the 45° than for the 90°, 135° and 180° groups. No statistical difference was found between the 135° and 180° groups. Taken together, these results indicate that it takes longer to adapt to large delays (135° and 180° groups) for which impact occurs during the physical racket downswing. Stability is completely lost in these conditions and phase space must be explored to identify and stabilize a new preferred phase.

We also investigated the proportion of impacts that occurred when the virtual racket was in the theoretical ‘passive stability regime’, in the active stabilization regime, or outside them in an uncontrolled region. Indeed, assuming sinusoidal racket motion, the racket

impact phase interval corresponding to the passive stability regime can be computed as follows:

$$\phi_v \in \left[ 90; 90 + \arctan \left( \left( \frac{2}{\pi} \right) \times \left( \frac{1+a^2}{1-a^2} \right) \right) \right],$$

and corresponds to  $\phi_v \in [90; 136.7^\circ]$ . The interval corresponding to the active stability regime is the remaining part of upward virtual racket motion  $\phi_v \in [0; 90^\circ]$ . When considering impact phases in the physical racket  $\phi_p$ , these intervals were shifted by an amount equal to the relative phase between both rackets (e.g., for 45° group, the passive stability regime corresponded to  $\phi_p \in [90 + 45, 136.7 + 45^\circ]$ ). The proportion of impacts that occurred in the ‘uncontrolled’ regions could be deduced from the sum of passive and active region proportions. Statistics about areas visited across learning are detailed in Table 3.

*First-return map for  $\phi_p$*

Finally, we investigated the evolution of  $\phi_p$  within individual trials during the learning session by plotting the first-return map for each trial in Session 2. The  $\phi_p$  of impact  $i + 1$  was plotted as function of its value on the preceding impact  $i$  separately for each trial, as illustrated in Fig. 2e–h. This analysis allowed us to visualize how the  $\phi_p$  space was visited from bounce to bounce during learning, and thus how the space was sampled and a stable impact



**Table 3** Proportions of impacts occurring in the passive and active regimes during blocks 1, 5 and 10 in Session 2

Blocks of session 2	Passive stability regime			Active stabilization regime		
	Block 1 (%)	Block 5 (%)	Block 10 (%)	Block 1 (%)	Block 5 (%)	Block 10 (%)
45° Group	41.71	66.99	75.64	56.50	32.74	24.23
90° Group	12.99	27.60	30.96	53.93	58.90	57.81
135° Group	6.24	30.26	29.39	31.69	50.01	51.72
180° Group	13.38	31.01	42.36	17.95	35.63	38.36

phase emerged over trials. Successive impacts during the racket upswing appear in the lower left quadrant, successive impacts during the downswing in the upper right quadrant, and impacts at the bottom of the racket cycle ( $0^\circ = 360^\circ$ ) appear on the perimeter or in the corners. The dark squares in Fig. 2e–h indicate the passive stability region for each delay condition, the light squares indicate the active stabilization region, and the observed stability at the end of Session 1 is in the lower left quadrant near ( $90^\circ, 136.7^\circ$ ).

Figure 7 presents first-return maps for every trial in the  $90^\circ$  and the  $180^\circ$  delay conditions from two representative participants; successive impacts are connected by line segments. Note that a tight cluster of points indicates a consistent or stable phase, diagonal rows of successive points indicate phase drift, wide scatter indicates instability or loss of control, and jumps between corners reflect impacts stuck near the bottom of the racket cycle, where racket velocity is low. In both conditions, scatter is observed during the initial trials, but impacts tend to converge at a small cluster of points over succeeding trials. The stabilization occurs quite quickly in the  $90^\circ$ -delay condition, but impacts converge at the active (rather than passive) stability region slightly below, which keeps them in the familiar upswing of the physical racket. In the  $180^\circ$  delay condition, there is wide scatter and corner sticking for many trials, with occasional clusters in the lower left quadrant during the upswing (near the Session 1 attractor) or in the upper right quadrant during the downswing (near the new solution); this hints at bi-stability, but not within a single trial. These maps indicate a loss of control and irregular visiting of the  $\phi_P$  space, rather than a systematic search for a new solution. By trial 30, the new passive stability was discovered, and impacts gradually converged on it over the remaining trials. The analysis thus reveals the attraction of bouncing behavior toward preferred regions of the  $\phi_P$  space, suggesting that they serve as behavioral attractors.

Session 3: normal spatio-temporal congruency  
[relative phase ( $\Delta\phi$ ) =  $16^\circ$ ]

Session 3 was kept similar to Session 1, in order to check for after-effects of adaptation to the time delay during

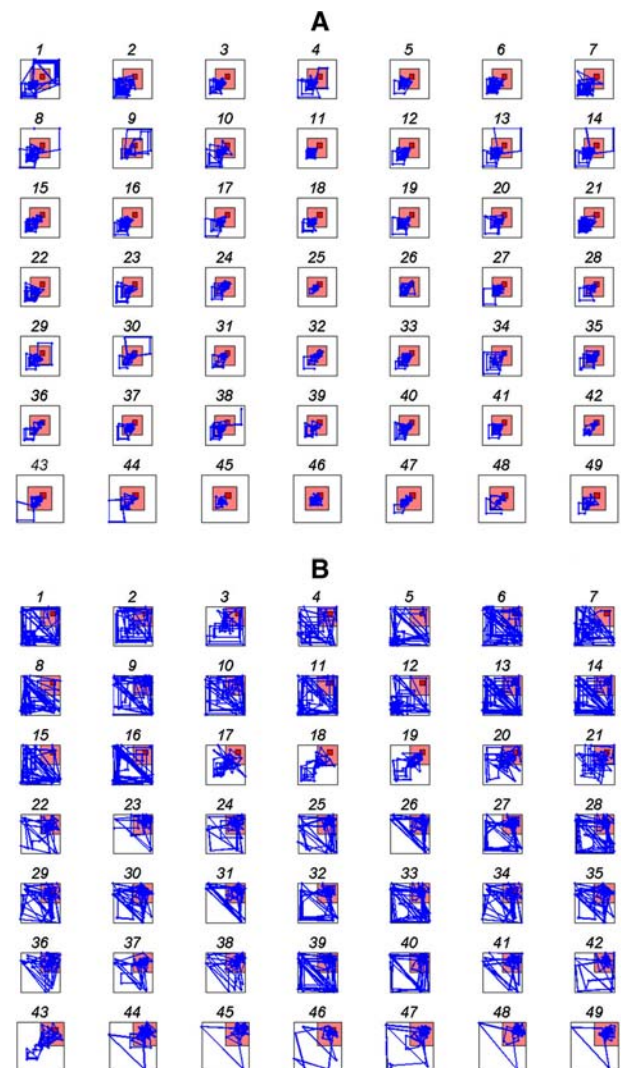


**Fig. 7** First return maps ( $\Phi_{P,i+1}$  vs.  $\Phi_{P,i}$ ) of two participants for 49 trials in Session 2. **a** One participant in the  $90^\circ$  condition. **b** One participant in the  $180^\circ$  condition. The 49 return maps are drawn for the entire space of  $\Phi_P$ , the racket phase at impact ( $360^\circ \times 360^\circ$ ). The winding line illustrates the evolution of  $\Phi_P$  for bounce  $i + 1$  against  $\Phi_P$  for bounce  $i$ , for every bounce in a trial. See text for details

Session 2, such as destabilization of bouncing behavior. Figs. 4 and 5 indicate an immediate recovery at the beginning of Session 3. However, all groups but the  $135^\circ$  delay group exhibited small but significant differences in

both performance ( $PER_V$  and  $ERR_B$ ) and impact variables ( $VEL_V$ ,  $ACC_V$ ,  $\phi_V$ ) in the first block of Session 3 when compared with the last block of Session 1 (paired samples  $t$ -test,  $P < 0.05$ ). Behavioral changes were found to occur within Session 3 for all groups and all variables. Indeed, ANOVAs (10 blocks  $\times$  4 groups) separately performed on  $PER_V$ ,  $ERR_B$ ,  $VEL_V$ ,  $ACC_V$  and  $\phi_V$  revealed that both performance and impact behaviors were significantly influenced by repetition,  $F_{(4,88)} > 3.85$ , all  $P < 0.05$ .

On the other hand, there were no significant group differences for the session means of  $PER_V$  or  $ERR_B$ , suggesting that the four groups had the same overall bouncing performance in Session 3. The same was true for means of  $VEL_V$ ,  $ACC_V$  and  $\phi_V$ , indicating that the impact behavior was also similar among groups. No significant Group  $\times$  Block interactions were found,  $F_{(12,88)} > 1.34$ , all  $P > 0.05$ , indicating that learning in Session 3 was similar for all groups. The overall mean  $ACC_V$  was equal to  $0.04 \pm 5.51 \text{ m/s}^2$  in the first block of Session 3 and to  $1.25 \pm 4.91 \text{ m/s}^2$  in the last block. In addition, all  $ACC_V$  values were significantly different from 0 ( $P > 0.05$ ). Thus, despite slight group differences at the beginning of Session 3, all groups rapidly recovered from the effects of adaptation to time delay.

## Discussion

In this article, we examined how naïve participants learned to perform regular bounces of a ball on a racket with an interactive virtual display in which time delays between the physical racket and the virtual racket were introduced. Our main focus of interest was how participants would identify and achieve new stable solutions for bouncing under these conditions.

Do participants exploit passive stability?

The results obtained for normal bouncing in Session 1 showed that good performance was achieved by all participants within 50 trials. However, contrary to the results reported by Sternad et al. (2001a), our data do not show a negative virtual racket acceleration at impact. Although a significant exponential decrease in acceleration was observed during Session 1, acceleration values at impact remained positive ( $3.18 \pm 5.38 \text{ m/s}^2$ ) rather than moving into the predicted passively stable range  $[-10.9, 0]$ . In the presence of added delays (relative phase) in Session 2, none of the final  $ACC_V$  values for the  $135^\circ$  and  $180^\circ$  groups were significantly different from  $0 \text{ m/s}^2$  whereas almost all  $ACC_V$  values for the  $45^\circ$  and  $90^\circ$  groups were significantly positive. Finally, mean  $ACC_V$  still remained slightly positive at the end of Session 3 ( $1.25 \pm 4.91 \text{ m/s}^2$ ).

Thus, although impact acceleration decreased with practice, observers did not achieve a passively stable solution in any condition. This result confirms earlier findings that bouncing can be maintained outside the passively stable regime, presumably by means of active control based on visual information about the ball's trajectory (de Rugy et al. 2003).

These non-negative  $ACC_V$  values can be attributed to a combination of three factors. First, the end-to-end latency of 29.73 m s in our VR set-up contributes to higher impact accelerations. In a recent methodological study (unpublished data), which included 14 expert participants with ten 20 s trials per delay condition in a random order, we observed that  $ACC_V$  increases linearly with delay whereas  $ACC_P$  decreases slightly. Extrapolating to a zero delay, the curves converge at an impact acceleration of  $-6 \text{ m/s}^2$ , well within the passively stable regime. These results suggest that a 29.73 m s latency could increase the impact acceleration by about  $3 \text{ m/s}^2$ . Second, the naïve participants in the present study also exhibited higher  $ACC_V$  values than experienced participants did in the methodological study, for the same delay conditions. This is consistent with the observed decrease in impact acceleration with learning (Sternad et al. 2001b). Finally, pacing by an external metronome also leads to higher impact acceleration. Sternad and Katsumata (2000) reported a higher and more variable impact acceleration when a metronome was used than Sternad et al. (2001a, b) found without a metronome. It is possible that constraining movements to an imposed period and height may elicit a greater active contribution to the control of the bouncing cycle. Taken together, these factors can account for the slightly positive  $ACC_V$  values observed in the present study.

Learning a new attractor

The addition of a delay between the physical and virtual racket motion in Session 2 effectively shifted the preferred impact phase by  $45^\circ$  to  $180^\circ$  later in the physical racket cycle. Our primary question was how participants find a new behavioral solution and re-establish a stable bouncing pattern. One might expect that the preferred impact phase with the virtual racket would correspond to a passively stable negative impact acceleration (Sternad et al. 2001a, b). As just noted, however, impact acceleration for the virtual racket never became significantly negative. The data indicate that, under the present constraints participants actively stabilized bouncing with a preferred virtual impact phase near  $90^\circ$  in all delay conditions. Thus, it appears that a new solution for regular bouncing in the physical racket cycle was defined at a phase of approximately  $90^\circ$  and the relative phase determined by the added delay.

The results clearly demonstrate that the addition of longer delays ( $135^\circ$  and  $180^\circ$ ) initially destabilized behavior, whereupon participants found and gradually homed in on a new behavioral solution. The histograms in Fig. 6 show that the sharp peak in physical racket phase observed in Session 1 was abolished by the addition of a long delay, and participants visited the full range of phases during the first blocks of Session 2. After two to three blocks of trials, however, a new peak began to emerge and sharpened into a clearly preferred phase over the next two blocks. Inspection of the first-return maps (Fig. 7) revealed a similar pattern on individual trials, such that during the first few blocks participants tended to jump about in phase from impact to impact, spanning the downswing as well as the upswing, and then intermittently began to cluster at a new preferred phase late in the downswing for an increasingly greater proportion of a trial. This pattern of results suggests that participants initially had difficulty in controlling bouncing after the introduction of a long delay, resulting in a broad sampling of phase during which a new solution was discovered and gradually stabilized. On the other hand, with shorter delays ( $45^\circ$  and  $90^\circ$ ) the unimodal distribution smoothly shifted to a new preferred phase later in the upswing. In the first return maps, phase jumping occurred only on the first few trials, and a tight clustering in phase quickly emerged.

It thus appears that participants could adapt to the shorter delays by simply shifting the impact phase later in the physical upswing, preserving the spatial symmetry between the ball's direction of motion and the physical racket's direction of motion at impact. In contrast, we suggest that the destabilization observed at longer delays is due to the fact that impact had to occur during the downswing of the physical racket, in order for the virtual racket to hit the ball on the upswing and maintain bouncing. This required stabilizing an unfamiliar perceptual-motor pattern that reversed the spatial relation between the ball and physical racket motions. It is likely that the visibility of the virtual racket (which preserved the normal symmetry) facilitated learning of the new coordination pattern (Mechsner et al. 2001).

The observed pattern of learning with longer delays, which involved the disappearance of one preferred phase followed by the emergence and progressive sharpening of another without systematic bistability, reflects the loss of stability in one perceptual-motor behavior and the stabilization of a new one (Zanone and Kelso 1992). The new solution can be interpreted as a "behavioral attractor" in the sense that participants converged on a preferred impact phase that reduced variability; more stringent tests of stability would include perturbations of the ball's trajectory (de Rugy et al. 2003). In the present case, broad sampling appears to be an effective process for exploring and iden-

tifying such a stable solution. Foo et al. (2004) observed a similar broad sampling of parameter space in infants learning to bounce in a baby bouncer. Values of leg stiffness and kicking frequency were widely scattered from bout to bout, and then suddenly converged on a preferred combination at the onset of stable bouncing. Such results suggest a non-systematic exploration of the variable space rather than a directed search for new behavioral attractors.

#### Delay and new sensory congruencies

The time delays introduced in Session 2 also modified the congruence between kinesthetic and visual feedback for racket motion, producing a sensory rearrangement. Welch (1978) described the overall pattern of adaptation to a new temporal sensory relationship as follows: (a) performance decrease; (b) performance increase after a few minutes of exposure; (c) strong aftereffect; (d) changes in the perceived relationship between the two sensory modalities; and (e) adaptation effects. The results presented in Session 3 failed to show the strong negative after effect on behavior expected by Welch's definition. Consequently, the observed changes during Session 2 do not seem to reflect an adaptation mechanism in the traditional sense. Two classes of difficulty for mismatch between kinesthetic action and delayed visual feedback have been identified for rhythmic tracking tasks (Langenberg et al. 1998): "easier" for delays between 0–30% and 90–105% of the tracking period and "harder" for delays between 30 and 90%. This seems to be consistent with the present results, for the  $45^\circ$  and  $90^\circ$  conditions should be classified as easier and the  $135^\circ$  and  $180^\circ$  conditions as harder. Moreover, Langenberg pointed out that the introduction of relative delay could lead to non-monotonic motor consequences. Indeed, he observed that RMS target errors first increased with small relative delays but decreased with relative delays close to a cycle period. Similarly, we found here evidence for a non-monotonic influence of the delay on behavior. Indeed, the time-dynamics of exponential fits on  $ERR_B$  changes during the learning session revealed a similar inverted U-shape function, with time constants equal to 2.36 blocks for the  $45^\circ$  group, 1.74 blocks for the  $90^\circ$  group, 4.99 blocks for the  $135^\circ$  group and 2.64 blocks for the  $180^\circ$  group. However, the increase in performance was here observed for relative delays close to a half cycle period. This result suggests that  $180^\circ$  relative phasing provides an inverse symmetry, probably of spatial origin, that appears helpful in learning new perception–action behaviors.

In the present experiment, adaptation seemed to take longer (more than 20 trials) for delays above 100 ms (relative phase  $> 45^\circ$ ). This result is consistent with the fact that human performance during initial exposure to a sensory rearrangement is known to be impaired. The

deterioration is caused by the new perceptual-motor coordination required by the end-to-end latency when using real time systems. This result is reported in many studies investigating the effect of delayed visual feedback (Wenzel 1998; Allison et al. 2001; Welch 1978), which have shown that the threshold at which visual lag started to affect performance was approximately 75 m s. According to Gobbeti and Scateni (1998), depending on task and environment, an end-to-end latency as small as 100 m s can reduce human performance, and if it goes beyond 300 m s, humans begin to separate action and its visual consequences. However, Cunningham et al. (2001) found that after 5–20 min of exposure to a 235 m s delay, performance in an interactive obstacle-avoidance task matched that with immediate feedback. Foulkes and Miall (2000) investigated the adaptation to visual feedback delays (200 and 300 m s) in a tracking task and found that performance clearly improved with practice. Moreover, they showed that the time to reach an appropriate adaptation was proportional to the magnitude of delayed visual feedback.

In our experiment, kinesthetic feedback arrived before visual feedback. Participants had to match the visual racket with the virtual ball while the match between kinesthetic and visual feedback of the racket was disrupted. Thus, to maintain bouncing a new sensory rearrangement had to be learned, which depended on the phase lag between physical and virtual racket. However, the consequence of the delay on performance did not seem to be directly proportional to the delay. Performance (time-course of learning) and impact behavior (dispersion of  $\phi_p$  and proportion of passive impacts) in the 180° group tended to reach a better level by the end of Session 2 than in the 135° group. The spatial regularities, expressed as relative phases (45°, 90°, 135°, 180°), seemed to have had some influence on the way participants learned the new perception action solutions.

## Conclusion

The present results demonstrate that, when faced with the destabilization of a preferred perceptual-motor pattern, humans respond by identifying a new behavioral solution. They appear to discover this new solution through wide exploration of the variable space and progressive stabilization of a new behavior pattern. This observation seems to verify Newell's (1991, 1989) definition of motor learning, described as a search for an optimal solution in the task space. Discoveries of new solutions here do not appear to result from a directed search but rather from a mechanism of random variation and selection. Such a mechanism bears an obvious resemblance to Darwin's (1859) theory of natural selection, or to genetic algorithms for efficient search (Holland 1992), and could be of a self-organized nature

(Cole 2002). Specifically, this involves (i) the production of a large variety of behaviors, in this case a wide dispersion of impact phases; and (ii) a selection mechanism based on behavioral success, in this case the selection of impact phases that yield stable bouncing. Under the present constraints, participants did not simply rely on passive stability to define a new solution, but rather a combination of passive and active stabilization based on perceptual information.

**Acknowledgments** Supported by the French Fond National pour la Science (IUF 2002:2006), and by Enactive Interfaces, a network of excellence (IST contract #002114) of the Commission of the European Community, with additional support from the University of Paris Sud 11 (BQR-RV-2003).

## References

- Adelstein BD, Johnston ER, Ellis SR (1996) Dynamic response of electromagnetic spatial displacement trackers. *Presence Teleoper Virtual Environ* 5: 302–318
- Allison RS, Harris LR, Jenkin M, Jasiobedzka U, Zacher JE (2001) Tolerance of temporal delay in virtual environments. *Virtual Reality 2001 conference (VR'01)*, Yokohama, pp 247–253, 17 March 2001
- Bingham GP, Schmidt RC, Zaal FT (1999) Visual perception of the relative phasing of human limb movements. *Percept Psychophys* 61:246–258
- Cole BJ (2002) Evolution of self-organized systems. *Biol Bull* 202:256–261
- Cunningham DW, Billock VA, Tsou BH (2001) Sensorimotor adaptation to violations of temporal contiguity. *Psychol Sci* 12:532–535
- Darwin C (1859) *On the origin of species by means of natural selection, or the preservation of favoured races in the struggle for life*. Murray, London
- Dijkstra TMH, Katsumata H, de Rugy A, Sternad D (2004) The dialogue between data and model: passive stability and relaxation behavior in a ball-bouncing task. *J Nonlin Stud* 11(3):319
- Eversheim U, Bock O (2001) Evidence for processing stages in skill acquisition: a dual-task study. *Learn Mem* 8:183–189
- Foo P, Goldfield EC, Kay B, Warren WH (2004) The dynamics of infant bouncing: retrospect and prospect. In: *Symposium at the International Society of Infancy Studies*, Chicago
- Foulkes AJ, Miall RC (2000) Adaptation to visual feedback delays in a human manual tracking task. *Exp Brain Res* 131:101–110
- Gibson JJ (1979) *The ecological approach to visual perception*. Lawrence Earlbaum Associates Inc., Boston
- Gobbeti E, Scateni R (1998) *Virtual reality: past, present and future*. *Stud Health Technol Inform* 58:3–20
- Holland JH (1992) *Adaptation in natural and artificial systems*. MIT Press, Cambridge
- Kelso JAS (1981) On the oscillatory basis of movement. *Bull Psychon Soc* 18:63
- Kelso JAS (1994) Informational Character of Self-Organized Coordination Dynamics. *Hum Mov Sci* 13:393–413
- Kelso JAS (1995) *Dynamic Patterns: The Self-Organization of Brain and Behavior*. MIT Press, Cambridge, Mass
- Kelso JAS, Fink PW, DeLaplain CR, Carson RG (2001) Haptic information stabilizes and destabilizes coordination dynamics. *Proc Biol Sci* 268:1207–1213



- Langenberg U, Hefter H, Kessler KR, Cooke JD (1998) Sinusoidal forearm tracking with delayed visual feedback. I. Dependence of the tracking error on the relative delay. *Exp Brain Res* 118:161–170
- Liu YT, Mayer-Kress G, Newell KM (2003) Beyond curve fitting: a dynamical systems account of exponential learning in a discrete timing task. *J Mot Behav* 35:197–207
- Mechsner F, Kerzel D, Knoblich G, Prinz W (2001) Perceptual basis of bimanual coordination. *Nature* 414:69–73
- Newell KM, van Emmerik REA, McDonald PV (1989) Search strategies and the acquisition of coordination. In: Wallace SA (ed) *Perspectives on the coordination of movement*. Martinus Nijhoff, Dordrecht, pp 85–122
- Newell KM, McDonald MP, Kugler PN (1991) The perceptual-motor workspace and the acquisition of skill. In: Requin J, Stelmach GE (eds) *Tutorials in motor neuroscience*. Martinus Nijhoff, Dordrecht, pp 95–108
- Newell KM, Liu YT, Mayer-Kress G (1997) The sequential structure of movement outcome in learning a discrete timing task. *J Mot Behav* 29:366–282
- de Rugy A, Wei K, Muller H, Sternad D (2003) Actively tracking ‘passive’ stability in a ball bouncing task. *Brain Res* 982:64–78
- Saltzman E, Kelso JAS (1987) Skilled actions: a task-dynamic approach. *Psychol Rev* 94:84–106
- Schaal S, Atkeson CG, Sternad D (1996) One-handed juggling: a dynamical approach to a rhythmic movement task. *J Mot Behav* 28:165–183
- Schmidt RC, Carello C, Turvey MT (1990) Phase transitions and critical fluctuations in the visual coordination of rhythmic movements between people. *J Exp Psychol Hum Percept Perform* 16:227–247
- Siegler I, Mantel B, Warren WH, Bardy B (2003) Behavioral dynamics of a rhythmic ball-bouncing task. Paper presented at the IV progress in motor control conference, Caen, France
- Sternad D, Katsumata H (2000) The role of dynamic stability for the acquisition and performance of a rhythmic skill. In: Raczek J, Waskiewicz Z, Juras G (eds) *Current research in motor control*. Interaktiv SC, Katowice
- Sternad D, Duarte M, Katsumata H, Schaal S (2001a) Bouncing a ball: tuning into dynamic stability. *J Exp Psychol Hum Percept Perform* 27:1163–1184
- Sternad D, Duarte M, Katsumata H, Schaal S (2001b) Dynamics of a bouncing ball in human performance. *Phys Rev E Stat Nonlin Soft Matter Phys* 63:011902
- Tass P, Kurths J, Rosenblum MG, Guasti G, Hefter H (1996) Delay-induced transitions in visually guided movements. *Phys Rev E Stat Phys Plasma Fluids Related Interdiscip Topics* 54:R2224–R2227
- Warren WH (2006) The dynamics of perception and action. *Psychol Rev* 113:358–389
- Welch RB (1978) *Perceptual modification: adapting to virtual environment*. Academic, New York
- Wenzel EM (1998) The impact of system latency on dynamic performance in virtual acoustic environments. *Proceedings of the 15th International Congress on Acoustics Meeting of the Acoustical Society of America*, Seattle
- Wilson AD, Bingham GP, Craig JC (2003) Proprioceptive perception of phase variability. *J Exp Psychol Hum Percept Perform* 29:1179–1190
- Yamanishi J, Kawato M, Suzuki R (1980) Two coupled oscillators as a model for the coordinated finger tapping by both hands. *Biol Cyber* 37:219–225
- Zaal FT, Bingham GP, Schmidt RC (2000) Visual perception of mean relative phase and phase variability. *J Exp Psychol Hum Percept Perform* 26:1209–1220
- Zanone PG, Kelso JAS (1992) Evolution of behavioral attractors with learning: non-equilibrium phase transitions. *J Exp Psychol Hum Percept Perform* 18:403–421
- Zanone PG, Kelso JAS (1997) Coordination dynamics of learning and transfer: collective and component levels. *J Exp Psychol Hum Percept Perform* 23:1454–1480